Tellus B
Chemical and Physical Meteorology

Dimensionless Parameterizations of Air-Sea CO_2 Gas Transfer Velocity on Surface Waves

ORIGINAL RESEARCH PAPER

STOCKHOLM UNIVERSITY PRESS

SHUO LI
ALEXANDER V. BABANIN
CHANGLONG GUAN
*Author affiliations can be found in the back matter of this article

ABSTRACT

Accurate quantification of air-sea gas transfer velocity is critical for our understanding of air-sea CO_2 gas fluxes, global carbon budget and climate responses. CO_2 transfer velocity is predominantly subject to constraints of wave-related dynamic processes at the ocean surface layer but is typically parameterized with wind speed. This study proposes and compares two parameterizations which accommodate dimensionless wave terms. The validations are conducted using both laboratory and field measurements of CO_2 transfer and wave statistics. A scaling of bubble-mediated gas transfer is implemented into the formula that is linked to wave breaking probability. The improved parameterizations are capable of collapsing combined laboratory and field data sets which comprise diversified conditions of wind, wave and wave breaking.

CORRESPONDING AUTHOR:
Shuo Li
Department of infrastructure Engineering, University of Melbourne, Melbourne, Victoria, Australia
shuo.li6@unimelb.edu.au

KEYWORDS:
air-sea gas transfer; ocean surface waves; carbon dioxide; dimensionless parameterizations

TO CITE THIS ARTICLE:
Li, S, Babanin, AV and Guan, C. 2023. Dimensionless Parameterizations of Air-Sea CO_2 Gas Transfer Velocity on Surface Waves. *Tellus B: Chemical and Physical Meteorology,* 75(1), 1–12. DOI: https://doi.org/10.16993/tellusb.1867

1 INTRODUCTION

Cumulative anthropogenic Carbon Dioxide (CO_2) emissions have been considered responsible for global warming and climate extreme events. The ocean is dynamically exchanging CO_2 with atmosphere and has taken up about 26% of total human activity-induced CO_2 emissions over the last decade (Friedlingstein et al. 2022). The air-sea CO_2 flux (F) in a bulk formula is generally expressed as a function of gas transfer velocity (K_{co_2}), aqueous solubility (s) and partial pressure difference across the air-water interface:

$$F = K_{CO_2} \cdot S \cdot \left(pCO_{2w} - pCO_{2a}\right), \qquad (1)$$

where pCO_{2w} and pCO_{2a} are CO_2 partial pressure in surface water and air, respectively. To reduce uncertainties in the estimation of air-sea CO_2 fluxes for global carbon budget, high-quality data sets of CO_2 partial pressure and accurate parameterizations for quantifying gas transfer velocity are required. Major advances have been made in collecting (Bakker et al. 2016; Takahashi et al. 2019) and reconstructing (e.g., Landschützer et al. 2020) observed ocean surface CO_2 concentration. The data sets with improved accuracy and temporal and spatial coverage provided notable support for the assessment of decadal trends and variabilities of historical air-sea CO_2 fluxes (Landschützer et al. 2016; Friedlingstein et al. 2022).

CO_2 transfer velocity K_{co_2} depends on environmental forcings including wind, surface waves, bubbles, surfactants, etc. The parameterizations of K_{co_2} based on wind or wave parameters have been derived in previous theoretical, laboratory and field studies. Gas transfer velocity is inversely correlated with a total resistance which is the sum of gas and liquid resistances. Because CO_2 is sparingly soluble in water, transfer resistance lies mainly in the water side (Bolin 1960; Liss 1973). Molecular diffusion (for tranquil water body) and turbulent mixing in water boundary layer are dominant mechanisms for transfer efficiency. Considering that the kinetic energy input to water is originated from wind stress, typical parameterizations of K_{co_2} are developed in terms of wind speed (U^m) with power m ranging from 1 to 3. For example, by employing laboratory and field (lake) observations, Liss and Merlivat (1986) proposed a piecewise linear function regarding smooth water surface, wavy surface and wave breaking surface under varied wind regimes. Thereafter, quadratic dependences were developed to estimate K_{co_2} under intermediate wind speed (Wanninkhof 2014; Nightingale et al. 2000; Ho et al. 2006). For high wind speed with wave breaking and bubble entrainment, cubic relationship was adopted (Wanninkhof and McGillis 1999). With the development of eddy-covariance method for ocean observations, the gas transfer velocity with wind speed has been actively investigated (McGillis et al. 2001; Miller et al. 2010; Landwehr et al. 2018; Dong et al. 2021; Yang et al. 2022). It is also worth noting that in laboratory, K_{co_2} was also measured under extreme wind conditions with 10m wind speed (U_{10}) up to 70 *m/s* by Iwano et al. (2013) and 85 *m/s* by Krall et al. (2019). They established a new regime of U_{10} beyond 33 *m/s* in which K_{co_2} was largely enhanced. The magnitude of power of wind speed and constants used in previous wind-based formulae were tuned for a mean dependence of K_{co_2} on wind speed. These empirical relationships can yield reasonable K_{co_2} estimations within their scope of validity but have uncertainties induced by complex physical processes in water (e.g. wave breaking, bubbles). Gaps exist across the formulae especially under intermediate to high winds (Wanninkhof 2014; Zhao et al. 2003), which reveals the inadequacy of wind-only parameterizations.

For CO_2 gas transfer, the turbulent intensity in water is of vital importance. With the wind stress acting on sea surface, a part of wind energy is transferred directly to the drift currents through viscous stress while the other part supplies the growth of waves. By applying a rigid boundary and assuming that turbulent dissipation is balanced by the shear production, a "wall layer" with constant stress and logarithmic velocity profile exists at water surface. Turbulent kinetic energy (TKE) in this layer can be simply scaled with the cube of the water-side friction velocity and the TKE dissipation rate is inversely proportional to the depth (Craig and Banner 1994). However, near-surface turbulence can be significantly enhanced by waves and wave breaking. It has been proposed (Qiao et al. 2004; Babanin 2006) and verified (Babanin and Haus 2009; Dai et al. 2010; Babanin and Chalikov 2012) that waves, even without breaking, can produce turbulence through wave orbital motions when water-side Reynolds number exceeds a critical value. The turbulence induced by non-breaking waves can be effectively strong and affect other ocean processes such as the upper-ocean mixing (Toffoli et al. 2012). In spectral waves, energy is transferred among the wave scales (i.e. wavenumbers) through nonlinear wave-wave interactions and subsequently dissipates via wave breaking, the processes of which are in balance with the wind input in equilibrium range of wave spectrum (Phillips 1985). Recognizing the important role of waves and wave breaking for TKE, the vertical profile of TKE dissipation rate and its wave-dependent scaling have been studied (Terray et al. 1996; Babanin et al. 2005; Gemmrich 2010; Sutherland and Melville 2015; Thomson et al. 2016; Lee et al. 2017).

In addition to the turbulence, wave breaking also generates bubble plumes which offer extra interface with increased partial pressure in bubbles and are important especially for sparingly soluble gases (Bell et al. 2017). The behavior of injected bubbles is subject to the turbulence in the vicinity. Melville et al. (1992) found that up to 50% of the dissipated energy from wave breaking could be expended on air entrainment against buoyancy forces. The large bubbles are broken up into smaller ones by turbulent fluctuations. This process stops at the Hinze scale (Hinze 1955; Garrett et al. 2000) at which surface tension of bubbles prevents further breakup. Through dimensional analysis, Garrett et al. (2000) proposed that the bubble size spectrum was related with local TKE dissipation rate, air supply rate and bubble radius. Deike et al. (2016) further parameterized the total air entrainment with breaking wave parameters for practical application.

The correlation between gas transfer velocity and wave-related dynamic processes (i.e. turbulence, bubbles) has been investigated by previous studies. Based on surface renewal theory, Lamont and Scott (1970) found that gas transfer velocity was proportional to TKE dissipation rate with a power of 0.25. This relationship has been supported by both theoretical and field studies (e.g., Lorke and Peeters 2006; Zappa et al. 2007). Jähne et al. (1987) suggested that mean square slope of the waves was a proper parameter to characterize gas transfer velocity. In laboratory, Zappa et al. (2001; 2004) observed that the fractional area coverage of microwave breakers under low to intermediate wind speed was another suitable parameter. At ocean surface, whitecaps are commonly observed in the process of wave breaking. Zhao et al. (2003) and Woolf (2005) employed whitecap coverage as a proxy to scale gas transfer velocity. Furthermore, whitecap coverage in these studies was scaled with a wind-sea Reynolds number rather than wind speed alone. The Reynolds number, denoted as R_H or R_B, is non-dimensional and can be written as

$$R_H = u_* H_S / v_a, \tag{2}$$

$$R_B = u_*^2 / \left(\omega_p v_a\right), \tag{3}$$

where u_* is wind friction velocity, H_s is significant wave height, ν_a is air kinematic viscosity, and ω_p is peak angular frequency of wave spectrum. R_H and R_B are interpreted as a measure of turbulence generated by wind waves and wave breaking. Their formulae imply that both wind force and sea state are equally important. Brumer et al. (2017) adapted the Reynolds number by changing ν_a to ν_w (water kinematic viscosity) and reconciled gas transfer data sets collected from field observations. Toba et al. (2006) discussed the similarity between air-sea momentum flux and gas flux, and proposed a non-dimensional treatment (divided by wind speed) for gas transfer velocity which was further correlated with the wind-sea Reynolds number. Li et al. (2021) observed the CO_2 gas transfer in laboratory under scenarios of mechanically-generated modulational wave trains without wind forcing, wind-generated waves and the combination of modulational waves and superimposed wind. They formulated non-dimensional parameterizations in which wave parameters were dominant.

Bubble-mediated gas transfer has been modeled and observed in previous studies (Woolf and Thorpe 1991; Keeling 1993; Woolf et al. 2007; Bell et al. 2017; Zavarsky et al. 2018) and is commonly scaled with the wind speed (Stanley et al. 2009; Liang et al. 2013) or whitecap coverage (Woolf 2005). Deike and Melville (2018) proposed a spectral framework for bubble-mediated gas transfer, in which wind friction and significant wave height were used. Based on this formula, Reichl and Deike (2020) estimated that global CO_2 gas fluxes via bubbles accounted for 40% of the total air-sea fluxes.

In the present study, we propose wave-dominated formulae and conduct validations using combined laboratory and field data. A simple bubble-mediated gas transfer scaling is obtained through field measurements and integrated into our formula. In addition, the efficiency of previous parameterizations is evaluated.

2 DATA AND METHODS

Synchronous measurements of gas transfer and environmental forcings from four field projects are collected in this study. To avoid the inconsistency caused by different observational methods, air-sea CO_2 fluxes across the projects were obtained through direct eddy-covariance measurements and the surface elevation for wave field was measured by Riegl laser altimeter. The air-sea CO_2 partial pressure was recorded by similar underway equilibrator system (e.g., (Pierrot et al. 2009). The local wind speed was measured by sonic anemometer. In addition, the ship motion, air and water temperature, air pressure and relative humidity (RH) were synchronously recorded during those campaigns. Except for the adopted hourly results from previous studies, variables are calculated in 10-minute segments with 50% overlap, which results in 11 pieces in one hour. Then the segments are averaged hourly to reduce the instability and deviation. The hourly results are further averaged into equidensity bins containing 15 data points.

The Southern Ocean Gas Experiment (SOGASEX) was conducted in Southern Ocean near South America from February to April in 2008 (Figure. 1 (*a*)). The region was selected for large air-sea CO_2 partial pressure difference to ensure a high signal-to-noise ratio of the eddy-covariance flux. CO_2 flux was measured by both closed and open path nondispersive infrared gas analyzers (NDIR). The 10m wind speed was up to about 20 *m/s* with mean value of 9.7 *m/s* (Edson et al. 2011). The mean RH was 87% and more than 25% of records were higher than 96% which is the upper limit of reliable RH measurements used. The final CO_2 transfer velocity computed following equation (1) is provided by Brumer et al. (2017).

The High Wind Gas Exchange Study (HIWINGS) took place at Labrador Sea from October to November in 2013

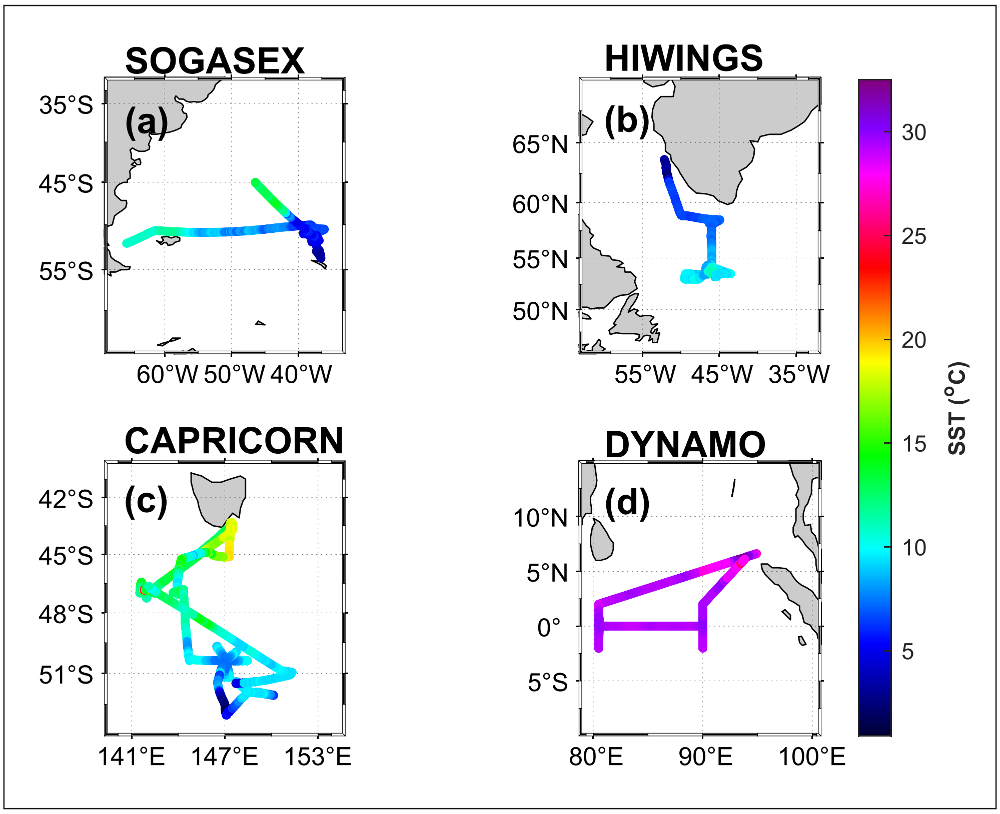

Figure 1 Cruise tracks and sea surface temperature along the tracks of **(*a*)**, SOGASEX project in Southern Ocean in year 2008; **(*b*)**, HIWINGS project at Labrador Sea in 2013; **(*c*)**, CAPRICORN project in Southern Ocean in 2016; **(*d*)**, DYNAMO project in Indian Ocean during 2011–2012.

(Figure 1 (*b*)). The region at that period was subject to high wind speeds, frequent storms and a well-known sink for atmospheric CO_2 with large partial pressure gradient. The wind speed was up to about 25 *m/s*. The wave field was measured by a Riegl laser altimeter and a Datawell Waverider buoy (model DWR-G4). Bubbles were also measured by a bubble camera (for big bubbles) and a bubble resonator located on spar buoy (for small-sized bubbles). Bubble measurement was operated for 40-minute duration at 3-hour intervals over a maximum of 48 hours in a single deployment. The CO_2 transfer velocity and bubble injection rate are provided by Blomquist et al. (2017).

CO_2 gas transfer was also measured in the project CAPRICORN during the Voyage IN2016_V02 from March to April 2016 in Southern Ocean near Australia (Figure 1 (*c*)). This project aims to explore Southern Ocean cloud systems, aerosol properties, surface energy budget, upper ocean biological aerosol production, and atmospheric composition. CO_2 flux was measured along the campaign through open path NDIR (LI-COR, LI-7500). CO_2 partial pressure was continuously measured by using a General Oceanic/Neill system which was equipped with a NDIR (LI-COR, LI-7000), shower head equilibrator and Nafion Dryer (Moreau et al. 2017). The wind speed was up to about 25 *m/s*. The wave field was also monitored through a Riegl laser altimeter. The observed CO_2 flux was processed following the method used by Blomquist et al. (2017).

DYNAMO program (Figure 1 (*d*)) was conducted during year 2011–2012 in tropical Indian Ocean where Madden Julian Oscillation (MJO) as a result of ocean atmosphere interaction can affect the earth's climate. The ocean in this region was a weak source for atmospheric CO_2 with highest wind speed up to about 15 *m/s*. CO_2 flux was measured by both closed (LI-7200) and open (LI-7500) path NDIR. In this work, we employed the results from one LI-7500. The assessment of CO_2 flux follows Blomquist et al. (2014). CO_2 partial pressure was monitored through a system comprising an equilibrator, a CO_2 analyzer (LI-COR 840) and a Nafion air dryer.

Laboratory measurements of CO_2 transfer under different wind and wave conditions from Li et al. (2021) are also used to evaluate parameterizations. The experiment was designed to explore the role of waves in air-water CO_2 gas exchange. Three types of waves were forced in a flume including modulational wave trains generated by mechanical wave maker, pure wind waves and the superposition of mechanical waves and wind waves. Surface elevation was recorded by wave gauges. Wave breaking was also captured by cameras. CO_2 was measured by Apollo system (model AS-P2) which incorporated a shower head equilibrator, a multiposition valve, and a CO_2 analyzer (CRDS, model G2301 by Picarro). The wave sizes in the laboratory are evidently smaller than that observed in ocean. An appropriate non-dimensional scheme should be able to reconcile all data sets.

2.1 ASSESSMENT OF WAVE AND WIND PARAMETERS

Based on the records from Riegl laser altimeter, we can obtain ocean surface elevation data. Individual waves are recognized through upcrossing points referenced to the mean water surface. Wave height (from crest to trough) and wave length (stokes wave length computed from wave period) can be used for the computation of wave steepness. By employing the characteristic of wave breaking (Babanin et al. 2010; Toffoli et al. 2010), waves with steepness ε (=*ak*, *a* is wave amplitude, *k* is wave number) larger than 0.44 are recognized as breakers. The breaking probability (b_T) is then estimated as the ratio of the number of breakers to all waves. Statistical wave parameters such as wave height and period are computed through the analysis of 1-dimensional frequency spectrum. The significant wave height $H_S = 4\sqrt{m_0}$, where m_0 is zero-order spectral moment. The mean wave period T_{02} is computed as $\sqrt{m_0 / m_2}$, where m_2 is second order spectral moment.

The 10 m wind speed and wind friction velocity are obtained from COARE (version 3.5) model (Fairall et al. 2011) output in the analysis of campaign data. The computation of wind friction velocity depends on the choice of drag coefficient. In the present work, the wind speed component in our equation is at least one order less than the dominant term of waves. Therefore, the uncertainties in wind friction estimations could barely influence the results.

2.2 PARAMETERIZATIONS FOR CO_2 TRANSFER VELOCITY

Li et al. (2021) developed both non-dimensional gas transfer velocity ($\tilde{K}$) and Reynolds number (R_{HM} and R_{HB}) with wave parameters based on laboratory experiments. Their proposed parameterizations are:

$$\tilde{K} = \alpha \cdot (R_{HM} \cdot (1 + \tilde{U}))^{\beta}, \tag{4}$$

$$\tilde{K} = \alpha \cdot (b_T \cdot R_{HB} \cdot (1 + \tilde{U}))^{\beta}, \tag{5}$$

where α and β are fitting coefficients, 1 + $\tilde{U}$ is an enhancement factor (also dimensionless) representing additional wind effect, b_T in equation (5) is the wave breaking probability. In these equations, $\tilde{K}$ is expressed as

$$\tilde{K} = K_{600} / U_{wm}, \tag{6}$$

where K_{600} denotes the local gas transfer velocity (K_{CO_2}) being corrected to 20°C fresh water using Schmidt number *Sc* (K_{CO_2}/K_{600} = $(Sc_{CO_2}/Sc_{600})^{-0.5}$), $U_{wm} = \overline{a\omega}$ represents mean wave orbital velocity, ω is angular frequency. It should be noted that the wave orbital velocity, rather than wind speed (Toba et al. 2006), is employed as the characteristic velocity in the scaling of K_{600}, which reflects the considerations of TKE enhancement by wave breaking and transport by wave orbital motions (Anis and Moum 1995; Thomson et al. 2016). The wave Reynolds number R_{HM} in equation (4) can be written as

$$R_{HM} = H_S U_{wm} / v_w, \tag{7}$$

R_{HB} has the same form with R_{HM} but uses wave breaker's height and orbital velocity. The factor $\tilde{U}$ in equation (4) and (5) is expressed as

$$\tilde{U} = u_* / \sqrt{gH_s}, \tag{8}$$

where *g* is gravitational acceleration. $\tilde{U}$ is analogous to the inverse of wave age (c_p/u_*), except that c_p is replaced with a preferable parameter $\sqrt{gH_s}$ in $\tilde{U}$ (Lenain and Melville 2017).

The implications of Equation (4) and (5) are threefold: First, the equations are non-dimensional and have potential application to different wave scales in ocean; Second, gas transfer velocity is directly governed by wave components R_{HM} or b_T R_{HB} whereas 1 + $\tilde{U}$ is an enhancement term implying the secondary role of wind. 1 + $\tilde{U}$ will converge to 1 under no-wind circumstances but waves (e.g. swells) and wave breaking can still exist without wind; Third, equation (5) specifically emphasizes the contributions of wave breaking by including parameter b_T. It should be noted that bubble-mediated gas transfer is not explicitly accounted in equation (5).

In practical application to ocean observations in this study, we make three pre-adjustments for the equations. First, K_{600} in equation (6) is replaced with K_{600} which denotes the gas transfer velocity at 20°C sea water (K_{CO_2}/K_{660} = $(Sc_{CO_2}/Sc_{660})^{-0.5}$). Second, U_{wm} in equation (6) and (7) is computed through spectral parameters H_s and T_{02}, i.e. $U_{wm} = 4\pi\sqrt{m_2}$. Third, because the wave height and orbital velocity at breaking onset (for computing R_{HB}) are difficult to be estimated from field observations, we cautiously replace R_{HB} in equation (5) with R_{HM}. R_{HB} may be positively correlated with R_{HM} through the measurements by Li et al. (2021) (not presented here) while in fact their relationship should be complicated (see, for example, the distribution of breaking wave height reviewed by Babanin (2011)). Thus, equation (5) can be rewritten as

$$\tilde{K} = \alpha \cdot (b_T \cdot R_{HM} \cdot (1 + \tilde{U}))^{\beta}. \tag{9}$$

Equation (4) and (9) will be tested and improved with data sets obtained in laboratory and ocean campaigns.

3 REVISED PARAMETERIZATIONS FOR CO_2 TRANSFER VELOCITY

The evaluations of equation (4) and (9) are presented in Figure 2 (*a*) and (*b*). The error bars denote standard deviation from the average of binned data. In panel (*a*), equation (4) is able to collapse all data well although scatters still exist. The fitting coefficients α and β are modified as 9.57 · 10^{-11} and 0.876, respectively. The coefficient of determination (r^2) and root-mean-square

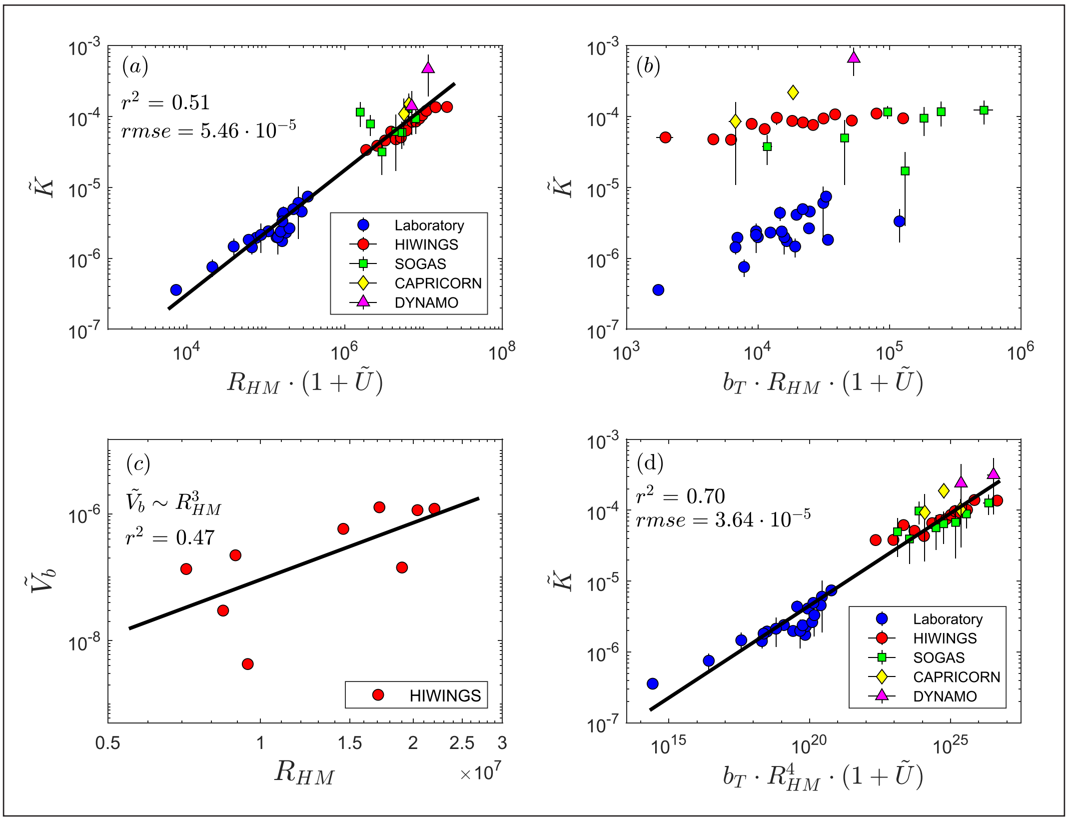

Figure 2 Dimensionless CO_2 transfer velocity $\tilde{K}$ versus **(*a*)**, $R_{HM} \cdot (1+\tilde{U})$ in equation (4); **(*b*)**, $b_T \cdot R_{HM} \cdot (1+\tilde{U})$ in equation (9); **(*d*)**, b_T $b_T \cdot R^4_{HM} \cdot (1+\tilde{U})$ in equation (10). Panel **(*c*)** shows the cubic relationship between dimensionless bubble injection rate $\tilde{V}_b = V_b/U_{wm}$ and R_{HM} based on the measurements from HIWINGS.

error (*rmse*) are also computed. Laboratory data (blue circles) are particularly in a good agreement with HIWINGS observations (red circles), for which r^2 is high as 0.96 (not presented). The scatter is mainly introduced by SOGASEX (green squares) and DYNAMO data (pink triangles) of which the deviations denoted by error bars are also relatively significant. Equation (9) in panel (*b*) apparently fails to reconcile all data sets. Gas transfer velocity from field observations are higher than the laboratory measurements under similar forcings computed by equation (9). The initial motivation for formulating equation (9) in laboratory is to highlight the importance of wave breaking. Gas transfer rate is regulated by the frequency of breaking events (b_T). However, R_{HM} is interpreted as an indicative turbulence parameter without accounting for the bubble's contribution (Li et al. 2021). Bubble-mediated gas transfer could be more evident in ocean than in laboratory because the magnitude of wave breaking in ocean can be larger. Thus, we propose to introduce bubble's effect into equation (9). Because the injected bubble volume and size distribution are closely correlated with environmental turbulence, it was suggested that bubble volume could be scaled with wave breaking dissipated energy (Fairall et al. 2011; Long et al. 2011). Based on the bubble injection rate V_b (unit *m/s*) from HIWINGS, we can simply parameterize it with R_{HM}. From dimensional considerations, V_b is firstly scaled with wave orbital velocity U_{wm} (*m/s*) and the dimensionless injection rate is denoted as $\tilde{V}_b$. $\tilde{V}_b$ is found proportional to R^3_{HM} in Figure 2 (*c*). Although the correlation is evident (78%, not shown), r^2 is 0.47 with limited data points. Then, the bubble's effect in terms of R^3_{HM} is incorporated into equation (9) and the new formula is written as

$$\tilde{K} = \alpha \cdot (b_T \cdot R^4_{HM} \cdot (1+\tilde{U}))^\beta, \qquad (10)$$

where R_{HM} has a total power of 4. Figure 2 (*d*) shows a substantial improvement for equation (10) in reconciling all data. Computed r^2 is 0.7, higher than that of equation (4) in panel (*a*). The adjusted fitting coefficient α and β are computed as $2.82 \cdot 10^{-11}$ and 0.260, respectively.

With the collected data, we can also evaluate other dimensional parameterizations for CO_2 transfer velocity. In Figure 3 (*a*), evaluations of several popular wind-only formulae (Liss and Merlivat 1986; Wanninkhof 2014; Nightingale et al. 2000; McGillis et al. 2004; Edson et al. 2011) are presented. Although these formulae generally comply with field observations, they can not reduce the disparities between field and laboratory results. Indeed, even for measurements of two groups of experiments (blue and green circles) in laboratory, different wave states result in clear gaps under similar wind speeds. The results of DYNAMO (pink triangles) also show significant deviations from the predictions of wind-based formulae. The combined evidences could demonstrate the insufficiency of wind-only schemes. The hybrid parameter R_H in equation (2) is evaluated in Figure 3 (*b*). We also

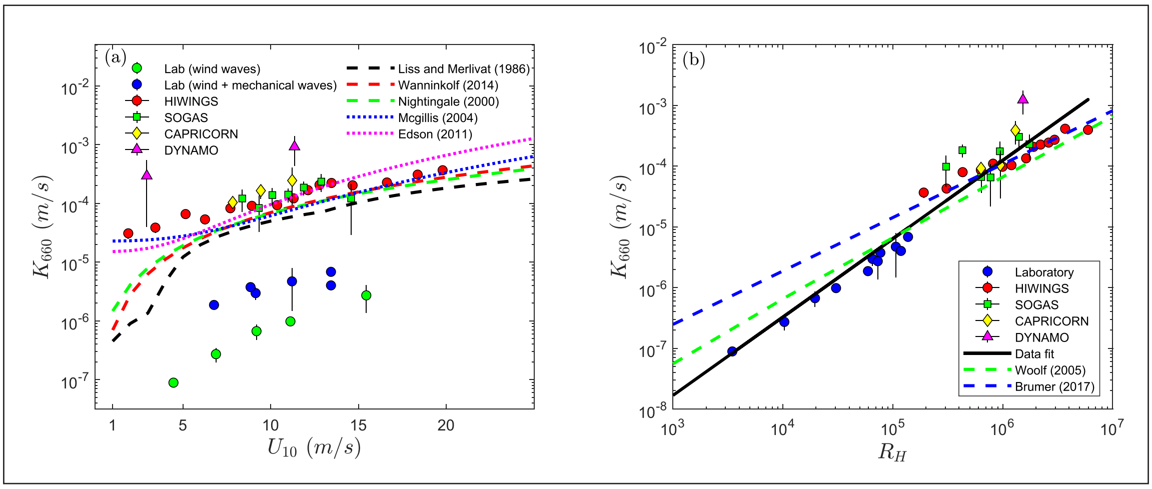

Figure 3 ***(a)***, dimensional CO_2 transfer velocity K_{660} versus 10m wind speed and predictions of wind-only parameterizations. ***(b)***, K_{660} versus the hybrid parameter R_H in equation (2). In panel ***(b)***, black solid line denotes the fitting result of all data. Blue and green dashed lines represent R_H parameterizations proposed by Brumer et al. (2017) and Woolf (2005), respectively.

demonstrate the transfer velocity predicted by R_H-based formulae from Brumer et al. (2017) and Woolf (2005) in panel *(b)*. Woolf (2005) divided the full expression of gas transfer velocity into two parts which comprised non-breaking and wave breaking contributions. R_H was used for characterizing wave breaking contribution while the non-breaking formula was a linear function of wind friction velocity. We compute the total transfer velocity (green dashed line) here and the non-breaking contribution becomes insignificant under intermediate to high wind speeds (not presented). R_H in panel *(b)*, to some extent, can collapse the data sets and the fitting result (black solid line) is close to the predictions of R_H-based formulae (blue and green dashed lines). However, these formulae capture relatively low variabilities. The computed r^2 are 25% and 27% for equations from Brumer et al. (2017) and Woolf (2005), respectively.

4 DISCUSSION AND CONCLUSION

The formulae (4) and (5) were initially developed in laboratory to account for the direct impacts of wave-related mechanisms on CO_2 gas transfer. They are fully dimensionless equations which are suitable for further application to open ocean conditions. With combined laboratory and field measurements, we adjusted and validated the formula (4). Its dominant term R_{HM} is built upon wave parameters and is a measure of wave induced turbulence (Babanin 2006). The effects of wind, on the other hand, is scaled as an enhancement factor ($\tilde{U}$) to account for the marginal contributions from the wind. We also established equation (10) to emphasize effects of wave breaking through probability b_T and bubble's contribution scaled with R_{HM}^3. The utilization of laboratory measurements provides the complement to diversified ocean wave conditions in the validation of our formulae. The formulae are also effective when they are evaluated with field observations. In Figure 4, we show an example of comparison between equation (4) and dimensional K_{660} correlated with 10 m wind speed by using HIWINGS observations. The fitting coefficient r^2 for equation (4) in panel *(a)* is higher than that for using wind speed in panel *(b)* (0.92 vs. 0.87). The obtained r^2 for equation (10) is 0.89 which also indicates a better fitting than that in panel *(b)*. In additon, similar conclusions can be achieved by using four field observations.

In this paper, b_T in equation (10) is estimated through wave measurements. But when it is not measured, parameterizations can be employed. b_T is determined by wave, wind and bottom-proximity properties. Banner et al. (2000) and Babanin et al. (2001) proposed dependences of b_T on significant wave steepness (ε) of the spectral peak in both deep and finite-depth water. Moreover, their studies show that the waves start to break ($b_T > 0$) when is higher than 0.055. The performance of equation (10) is limited under the condition of $b_T = 0$. Thus, equation (4) could be a supplement to equation (10) using the criteria of wave steepness,

$$\tilde{K} = \begin{cases} 9.57\cdot 10^{-11}\cdot (R_{HM}\cdot(1+\tilde{U}))^{0.876}, & \varepsilon \le 0.055 \\ 2.82\cdot 10^{-11}\cdot (bT\cdot R_{HM}^4\cdot(1+\tilde{U}))^{0.260}, & \varepsilon > 0.055 \end{cases} \quad (11)$$

The other motivation for proposing equation (11) is its potential application in modeling since the variables can be readily computed in spectral wave models (e.g., WAVEWATCH III (Rogers and Zieger 2014)).

The wave breaking induced air entrainment through bubbles may be more notable in open ocean than in laboratory wave tank because of the difference in wave scales and breaking strength. If the bubble's effect becomes evident for CO_2 transfer in ocean, it is reasonable that equation (10) captures more variabilities compared with equation (4). Due to the paucity of bubble measurements in this study, the power dependence of bubble injection rate on R_{HM} could be further improved with more data. Additionally, bubble-mediated gas

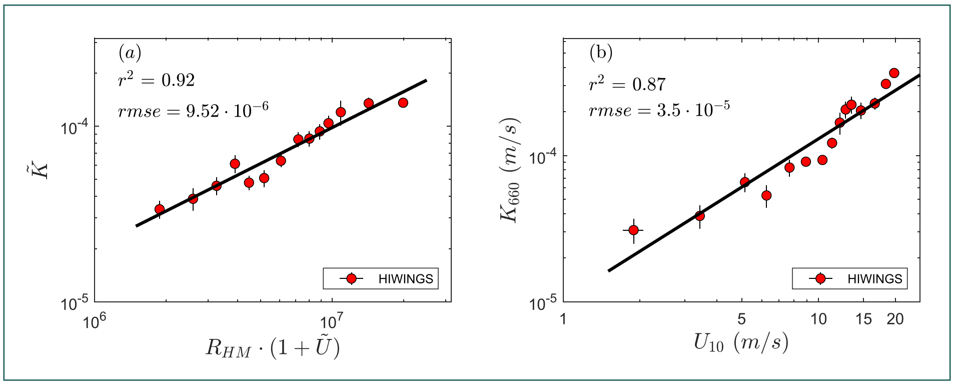

Figure 4 (*a*), Non-dimensional CO_2 transfer velocity $\tilde{K}$ versus $R_{HM} \cdot (1+ \tilde{U})$. **(*b*)**, Dimensional CO_2 transfer velocity K_{660} versus 10m wind speed. Black solid line in each panel is the result of log-log fit.

transfer is actually complicated, which is relevant with wave breaking strength (Manasseh et al. 2006), bubble injection depth, rise velocity and transfer rate for bubbles with different sizes (Woolf et al. 2007). Physical parameterizations for bubble-mediated transfer should be involved in the future study.

The results of DYNAMO project in our study have higher deviations than that of other projects, which could be attributed to low signal-to-noise ratio under mild wind and wave states. The observed partial pressure and fluxes for CO_2 are generally less significant than that of other cruises. Diurnal heat fluxes at daytime causing surface stratification and subsequent buoyancy fluxes at night (McGillis et al. 2004) are also important. These factors may all contribute to the deviation of predicted gas transfer velocity. CAPRICORN project was not specially designed for gas exchange experiment and only had one equipment for CO_2 flux. Thus, limited results are obtained after data processing. Our formulae only reflect the role of dynamic processes related with wind and wave, and can not represent other mechanisms that might significantly influence CO_2 gas fluxes, such as surfactants (Frew 1997) and rainfall (Takagaki and Komori 2007) which can suppress and intensify surface turbulence respectively. All the other influencing factors could lead to divergence of our formulae. In addition, the proposed parameterizations in this study are restricted to CO_2 or other sparingly soluble gases, rather than soluble gases. Air-side dynamics are the main constraint for soluble gas exchange, for which suitable parameterizations should be built upon wind parameters. Although Brumer et al. (2017) used a single parameter R_H (or R_B) and reconciled both CO_2 and DMS measurements, the obtained fitting may exhibit more discrepancies. The role of bubbles for gases with different solubilities needs to be properly represented in gas exchange scheme as well.

To summarize, CO_2 gas transfer models are proposed and validated through combined data from laboratory and field campaigns. Non-dimensional formulae (4), (10) and (11) depend on wave-related terms and can successfully bring together all data sets which span a wide range of wind and wave conditions. Bubble-mediated gas transfer is incorporated in formula (10), the performance of which is thus enhanced.

DATA ACCESSIBILITY STATEMENT

Data sets in this study are publicly available online. The laboratory data is available at Li et al. (2021); The field data from HIWINGS, CAPRICORN and DYNAMO campaigns can be found at ftp1.esrl.noaa.gov/psd3/cruises; The SOGASEX data can be accessed at http://www.bco-dmo.org/project/2064

ACKNOWLEDGEMENTS

S.L. and A.V.B. acknowledge support from the U.S. Office of Naval Research Grant N62909-20-1-2080. The authors thank Sophia E. Brumer for providing CO_2 transfer velocity of SOGASEX. The authors also appreciate the help from Byron Blomquist and Christopher Fairall for providing other ocean campaign data. The authors also thank Yuanxu Dong for providing valuable advices on manuscript.

COMPETING INTERESTS

The authors have no competing interests to declare.

AUTHOR AFFILIATIONS

Shuo Li orcid.org/0000-0002-9425-1040
Department of infrastructure Engineering, University of Melbourne, Melbourne, Victoria, Australia

Alexander V. Babanin orcid.org/0000-0002-8595-8204
Department of infrastructure Engineering, University of Melbourne, Melbourne, Victoria, Australia; Laboratory for Regional Oceanography and Numerical Modeling, National Laboratory for Marine Science and Technology, Qingdao, China

Changlong Guan
College of Oceanic and Atmospheric Sciences, Ocean University of China, Qingdao, China

REFERENCES

Anis, A and **Moum, JN.** 1995. Surface wave–turbulence interactions scaling ε (z) near the sea surface. *Journal of Physical Oceanography*, 25(9): 2025–2045. DOI: https://doi.org/10.1175/1520-0485(1995)025<2025:SWISNT>2.0.CO;2

Babanin, AV. 2006. On a wave-induced turbulence and a wave-mixed upper ocean layer. *Geophysical Research Letters*, 33(20). DOI: https://doi.org/10.1029/2006GL027308

Babanin, AV. 2011. *Breaking and dissipation of ocean surface waves*. Cambridge University Press. DOI: https://doi.org/10.1017/CBO9780511736162

Babanin, AV and **Chalikov, D.** 2012. Numerical investigation of turbulence generation in nonbreaking potential waves. *Journal of Geophysical Research: Oceans*, 117(C11). DOI: https://doi.org/10.1029/2012JC007929

Babanin, AV, Chalikov, D, Young, IR and **Savelyev, I.** 2010. Numerical and laboratory investigation of breaking of steep two-dimensional waves in deep water. *Journal of Fluid Mechanics*, 644: 433–463. DOI: https://doi.org/10.1017/S002211200999245X

Babanin, AV and **Haus, BK.** 2009. On the existence of water turbulence induced by nonbreaking surface waves. *Journal of Physical Oceanography*, 39(10): 2675–2679. DOI: https://doi.org/10.1175/2009JPO4202.1

Babanin, AV, Young, IR and **Banner, ML.** 2001. Breaking probabilities for dominant surface waves on water of finite constant depth. *Journal of Geophysical Research: Oceans*, 106(C6): 11 659–11 676. DOI: https://doi.org/10.1029/2000JC000215

Babanin, AV, Young, IR and **Mirfenderesk, H.** 2005. Field and laboratory measurements of wave-bottom interaction. *Proc. 17th Australasian Coastal and Ocean Engineering Conference and the 10th Australasian Port and Harbour Conference, 20–23 September 2005, Adelaide, South Australia*, 293–298.

Bakker, DC and **Coauthors.** 2016. A multi-decade record of high-quality fco (2) data in version 3 of the surface ocean co2 atlas (socat). *Earth System Science Data*, 8: 383–413. DOI: https://doi.org/10.5194/essd-8-383-2016

Banner, ML, Babanin, AV and **Young, IR.** 2000. Breaking probability for dominant waves on the sea surface. *Journal of Physical Oceanography*, 30(12): 3145–3160. DOI: https://doi.org/10.1175/1520-0485(2000)030<3145:BPFDWO>2.0.CO;2

Bell, TG and **Coauthors.** 2017. Estimation of bubble-mediated air–sea gas exchange from concurrent dms and co2 transfer velocities at intermediate–high wind speeds. *Atmospheric Chemistry and Physics*, 17(14): 9019–9033. DOI: https://doi.org/10.5194/acp-17-9019-2017

Blomquist, BW and **Coauthors.** 2017. Wind speed and sea state dependencies of air-sea gas transfer: Results from the high wind speed gas exchange study (hiwings). *Journal of Geophysical Research: Oceans*, 122(10): 8034–8062. DOI: https://doi.org/10.1002/2017JC013181

Blomquist, BW, Huebert, BJ, Fairall, CW, Bariteau, L, Edson, JB, Hare, JE and **McGillis, WR.** 2014. Advances in air-sea co2 flux measurement by eddy correlation. *Boundary-Layer Meteorology*, 152(3): 245–276. DOI: https://doi.org/10.1007/s10546-014-9926-2

Bolin, B. 1960. On the exchange of carbon dioxide between the atmosphere and the sea. *Tellus*, 12(3): 274–281. DOI: https://doi.org/10.3402/tellusa.v12i3.9402

Brumer, SE, Zappa, CJ, Blomquist, BW, Fairall, CW, Cifuentes-Lorenzen, A, Edson, JB, Brooks, IM and **Huebert, BJ.** 2017. Wave-related reynolds number parameterizations of co2 and dms transfer velocities. *Geophysical Research Letters*, 44(19): 9865–9875. DOI: https://doi.org/10.1002/2017GL074979

Craig, PD and **Banner, ML.** 1994. Modeling wave-enhanced turbulence in the ocean surface layer. *Journal of Physical Oceanography*, 24(12): 2546–2559. DOI: https://doi.org/10.1175/1520-0485(1994)024<2546:MWETIT>2.0.CO;2

Dai, D, Qiao, F, Sulisz, W, Han, L and **Babanin, AV.** 2010. An experiment on the nonbreaking surface-wave-induced vertical mixing. *Journal of Physical Oceanography*, 40(9): 2180–2188. DOI: https://doi.org/10.1175/2010JPO4378.1

Deike, L and **Melville, WK.** 2018. Gas transfer by breaking waves. *Geophysical Research Letters*, 45(19): 10–482. DOI: https://doi.org/10.1029/2018GL078758

Deike, L, Melville, WK and **Popinet, S.** 2016. Air entrainment and bubble statistics in breaking waves. *Journal of Fluid Mechanics*, 801: 91–129. DOI: https://doi.org/10.1017/jfm.2016.372

Dong, Y, Yang, M, Bakker, DC, Kitidis, V and **Bell, TG.** 2021. Uncertainties in eddy covariance air–sea co 2 flux measurements and implications for gas transfer velocity parameterisations. *Atmospheric Chemistry and Physics*, 21(10): 8089–8110. DOI: https://doi.org/10.5194/acp-21-8089-2021

Edson, J and **Coauthors.** 2011. Direct covariance measurement of co2 gas transfer velocity during the 2008 southern ocean gas exchange experiment: Wind speed dependency. *Journal of Geophysical Research: Oceans*, 116(C4). DOI: https://doi.org/10.1029/2011JC007022

Fairall, CW and **Coauthors.** 2011. Implementation of the coupled ocean-atmosphere response experiment flux algorithm with co2, dimethyl sulfide, and o3. *Journal of Geophysical Research: Oceans*, 116(C4). DOI: https://doi.org/10.1029/2010JC006884

Frew, N. 1997. The role of organic films in air-sea gas exchange. *The sea surface and global change*, 1249. DOI: https://doi.org/10.1017/CBO9780511525025.006

Friedlingstein, P and **Coauthors.** 2022. Global carbon budget 2021. *Earth System Science Data*, 14(4): 1917–2005. DOI: https://doi.org/10.5194/essd-14-1917-2022

Garrett, C, Li, M and **Farmer, D.** 2000. The connection between bubble size spectra and energy dissipation rates in the upper ocean. *Journal of physical oceanography*, 30(9): 2163–2171. DOI: https://doi.org/10.1175/1520-0485(2000)030<2163:TCBBSS>2.0.CO;2

Gemmrich, J. 2010. Strong turbulence in the wave crest region. *Journal of Physical Oceanography*, 40(3): 583–595. DOI: https://doi.org/10.1175/2009JPO4179.1

Hinze, JO. 1955. Fundamentals of the hydrodynamic mechanism of splitting in dispersion processes. *AIChE journal*, 1(3): 289–295. DOI: https://doi.org/10.1002/aic.690010303

Ho, DT, Law, CS, Smith, MJ, Schlosser, P, Harvey, M and **Hill, P.** 2006. Measurements of air-sea gas exchange at high wind speeds in the southern ocean: Implications for global parameterizations. *Geophysical Research Letters*, 33(16). DOI: https://doi.org/10.1029/2006GL026817

Iwano, K, Takagaki, N, Kurose, R and **Komori, S.** 2013. Mass transfer velocity across the breaking air–water interface at extremely high wind speeds. *Tellus B: Chemical and Physical Meteorology*, 65(1): 21 341. DOI: https://doi.org/10.3402/tellusb.v65i0.21341

Jähne, B, Münnich, KO, Bösinger, R, Dutzi, A, Huber, W and **Libner, P.** 1987. On the parameters influencing air-water gas exchange. *Journal of Geophysical Research: Oceans*, 92(C2): 1937–1949. DOI: https://doi.org/10.1029/JC092iC02p01937

Keeling, RF. 1993. On the role of large bubbles in air-sea gas exchange and supersaturation in the ocean. *Journal of Marine Research*, 51(2): 237–271. DOI: https://doi.org/10.1002/2016JC011744

Krall, KE, Smith, AW, Takagaki, N and **Jähne, B.** 2019. Air–sea gas exchange at wind speeds up to 85 m s-1. *Ocean Science*, 15(6). DOI: https://doi.org/10.5194/os-15-1783-2019

Lamont, JC and **Scott, D.** 1970. An eddy cell model of mass transfer into the surface of a turbulent liquid. *AIChE Journal*, 16(4): 513–519. DOI: https://doi.org/10.1002/aic.690160403

Landschützer, P, Gruber, N and **Bakker, DC.** 2016. Decadal variations and trends of the global ocean carbon sink. *Global Biogeochemical Cycles*, 30(10): 1396–1417. DOI: https://doi.org/10.1002/2015GB005359

Landschützer, P, Laruelle, GG, Roobaert, A and **Regnier, P.** 2020. A uniform pco 2 climatology combining open and coastal oceans. *Earth System Science Data*, 12(4): 2537–2553. DOI: https://doi.org/10.5194/essd-12-2537-2020

Landwehr, S, Miller, SD, Smith, MJ, Bell, TG, Saltzman, ES and **Ward, B.** 2018. Using eddy covariance to measure the dependence of air–sea co 2 exchange rate on friction velocity. *Atmospheric Chemistry and Physics*, 18(6): 4297–4315. DOI: https://doi.org/10.5194/acp-2017-861

Lee, J, Monty, J, Elsnab, J, Toffoli, A, Babanin, A and **Alberello, A.** 2017. Estimation of kinetic energy dissipation from breaking waves in the wave crest region. *Journal of Physical Oceanography*, 47(5): 1145–1150. DOI: https://doi.org/10.1175/JPO-D-16-0273.1

Lenain, L and **Melville, WK.** 2017. Measurements of the directional spectrum across the equilibrium saturation ranges of wind-generated surface waves. *Journal of Physical Oceanography*, 47(8): 2123–2138. DOI: https://doi.org/10.1175/JPO-D-17-0017.1

Li, S, Babanin, AV, Qiao, F, Dai, D, Jiang, S and **Guan, C.** 2021. Laboratory experiments on co 2 gas exchange with wave breaking. *Journal of Physical Oceanography*, 51(10): 3105–3116. DOI: https://doi.org/10.1175/JPO-D-20-0272.1

Liang, JH, Deutsch, C, McWilliams, JC, Baschek, B, Sullivan, PP and **Chiba, D.** 2013. Parameterizing bubble-mediated air-sea gas exchange and its effect on ocean ventilation. *Global Biogeochemical Cycles*, 27(3): 894–905. DOI: https://doi.org/10.1002/gbc.20080

Liss, PS. 1973. Processes of gas exchange across an air-water interface. *Deep Sea Research and Oceanographic Abstracts*, Elsevier, 20: 221–238, DOI: https://doi.org/10.1016/0011-7471(73)90013-2

Liss, PS and **Merlivat, L.** 1986. Air-sea gas exchange rates: Introduction and synthesis. *The role of air-sea exchange in geochemical cycling*, 113–127. Springer. DOI: https://doi.org/10.1007/978-94-009-4738-2_5

Long, MS, Keene, WC, Kieber, D, Erickson, D and **Maring, H.** 2011. A sea-state based source function for size- and composition-resolved marine aerosol production. *Atmospheric Chemistry and Physics*, 11(3): 1203–1216. DOI: https://doi.org/10.5194/acp-11-1203-2011

Lorke, A and **Peeters, F.** 2006. Toward a unified scaling relation for interfacial fluxes. *Journal of Physical Oceanography*, 36(5): 955–961. DOI: https://doi.org/10.1175/JPO2903.1

Manasseh, R, Babanin, AV, Forbes, C, Rickards, K, Bobevski, I and **Ooi, A.** 2006. Passive acoustic determination of wave-breaking events and their severity across the spectrum. *Journal of Atmospheric and Oceanic Technology*, 23(4): 599–618. DOI: https://doi.org/10.1175/JTECH1853.1

McGillis, WR and **Coauthors.** 2004. Air-sea co2 exchange in the equatorial pacific. *Journal of Geophysical Research: Oceans*, 109(C8). DOI: https://doi.org/10.1029/2003JC002256

McGillis, WR, Edson, J, Hare, J and **Fairall, C.** 2001. Direct covariance air-sea co2 fluxes. *Journal of geophysical research: Oceans*, 106(C8): 16 729–16 745. DOI: https://doi.org/10.1029/2000JC000506

Melville, WK, Loewen, M and **Lamarre, E.** 1992. Sound production and air entrainment by breaking waves: A review of recent laboratory experiments. *Breaking Waves*, 139–146. DOI: https://doi.org/10.1007/978-3-642-84847-6_11

Miller, SD, Marandino, C and **Saltzman, ES.** 2010. Ship-based measurement of air-sea co2 exchange by eddy covariance. *Journal of Geophysical Research: Atmospheres*, 115(D2). DOI: https://doi.org/10.1029/2009JD012193

Moreau, S and **Coauthors.** 2017. Eddy-induced carbon transport across the antarctic circumpolar current. *Global Biogeochemical Cycles*, 31(9): 1368–1386. DOI: https://doi.org/10.1002/2017GB005669

Nightingale, PD, Malin, G, Law, CS, Watson, AJ, Liss, PS, Liddicoat, MI, Boutin, J, and **Upstill-Goddard, RC.** 2000. In situ evaluation of air-sea gas exchange parameterizations using novel conservative and volatile tracers. *Global Biogeochemical Cycles*, 14(1): 373–387. DOI: https://doi.org/10.1029/1999GB900091

Phillips, OM. 1985. Spectral and statistical properties of the equilibrium range in wind-generated gravity waves. *Journal of Fluid Mechanics*, 156: 505–531. DOI: https://doi.org/10.1017/S0022112085002221

Pierrot, D and **Coauthors.** 2009. Recommendations for autonomous underway pco2 measuring systems and data-reduction routines. *Deep Sea Research Part II: Topical Studies in Oceanography*, 56(8–10): 512–522. DOI: https://doi.org/10.1016/j.dsr2.2008.12.005

Qiao, F, Yuan, Y, Yang, Y, Zheng, Q, Xia, C and **Ma, J.** 2004. Wave-induced mixing in the upper ocean: Distribution and application to a global ocean circulation model. *Geophysical Research Letters*, 31(11). DOI: https://doi.org/10.1029/2004GL019824

Reichl, BG and **Deike, L.** 2020. Contribution of sea-state dependent bubbles to air-sea carbon dioxide fluxes. *Geophysical Research Letters*, 47(9): e2020GL087267. DOI: https://doi.org/10.1029/2020GL087267

Rogers, WE and **Zieger, S.** 2014. New wave-ice interaction physics in wavewatch iii. Tech. rep., NAVAL RESEARCH LAB STENNIS DETACHMENT STENNIS SPACE CENTER MS OCEANOGRAPHY DIV.

Stanley, RH, Jenkins, WJ, Lott, DE, III and **Doney, SC.** 2009. Noble gas constraints on air-sea gas exchange and bubble fluxes. *Journal of Geophysical Research: Oceans*, 114(C11). DOI: https://doi.org/10.1029/2009JC005396

Sutherland, P and **Melville, WK.** 2015. Field measurements of surface and near-surface turbulence in the presence of breaking waves. *Journal of Physical Oceanography*, 45(4): 943–965. DOI: https://doi.org/10.1175/JPO-D-14-0133.1

Takagaki, N and **Komori, S.** 2007. Effects of rainfall on mass transfer across the air-water interface. *Journal of Geophysical Research: Oceans*, 112(C6). DOI: https://doi.org/10.1029/2006JC003752

Takahashi, T, Sutherland, SC and **Kozyr, A.** 2019. Global ocean surface water partial pressure of co2 database: Measurements performed during 1957–2018 (version 2018).

Terray, EA, Donelan, M, Agrawal, Y, Drennan, W, Kahma, K, Williams, AJ, Hwang, P and **Kitaigorodskii, S.** 1996. Estimates of kinetic energy dissipation under breaking waves. *Journal of Physical Oceanography*, 26(5): 792–807. DOI: https://doi.org/10.1175/1520-0485(1996)026<0792:EOKEDU>2.0.CO;2

Thomson, J, Schwendeman, MS, Zippel, SF, Moghimi, S, Gemmrich, J and **Rogers, WE.** 2016. Wave-breaking turbulence in the ocean surface layer. *Journal of Physical Oceanography*, 46(6): 1857–1870. DOI: https://doi.org/10.1175/JPO-D-15-0130.1

Toba,Y, Komori, S, Suzuki, Y and **Zhao, D.** 2006. Similarity and dissimilarity in air-sea momentum and co2 transfers: the nondimensional transfer coefficients in light of windsea reynolds number. *Atmosphere-ocean interactions*, 2: 53–82. DOI: https://doi.org/10.2495/978-1-85312-929-2/03

Toffoli, A, Babanin, AV, Onorato, M and **Waseda, T.** 2010. Maximum steepness of oceanic waves: Field and laboratory experiments. *Geophysical Research Letters*, 37(5). DOI: https://doi.org/10.1029/2009GL041771

Toffoli, A, McConochie, J, Ghantous, M, Loffredo, L and **Babanin, AV.** 2012. The effect of wave-induced turbulence on the ocean mixed layer during tropical cyclones: Field observations on the australian north-west shelf. *Journal of Geophysical Research: Oceans*, 117(C11). DOI: https://doi.org/10.1029/2011JC007780

Wanninkhof, R. 2014. Relationship between wind speed and gas exchange over the ocean revisited. *Limnology and Oceanography: Methods*, 12(6): 351–362. DOI: https://doi.org/10.4319/lom.2014.12.351

Wanninkhof, R and **McGillis, WR.** 1999. A cubic relationship between air-sea co2 exchange and wind speed. *Geophysical Research Letters*, 26(13): 1889–1892. DOI: https://doi.org/10.1029/1999GL900363

Woolf, DK. 2005. Parametrization of gas transfer velocities and sea-state-dependentwave breaking. *Tellus B: Chemical and Physical Meteorology*, 57(2): 87–94. DOI: https://doi.org/10.3402/tellusb.v57i2.16783

Woolf, DK and **Coauthors.** 2007. Modelling of bubble-mediated gas transfer: Fundamental principles and a laboratory test. *Journal of Marine Systems*, 66(1-4): 71–91. DOI: https://doi.org/10.1016/j.jmarsys.2006.02.011

Woolf, DK and **Thorpe, S.** 1991. Bubbles and the air-sea exchange of gases in nearsaturation conditions. *Journal of Marine Research*, 49(3): 435–466. DOI: https://doi.org/10.1357/002224091784995765

Yang, M and **Coauthors.** 2022. Global synthesis of air-sea co2 transfer velocity estimates from ship-based eddy covariance measurements. DOI: https://doi.org/10.3389/fmars.2022.826421

Zappa, CJ, Asher, W and **Jessup, A.** 2001. Microscale wave breaking and air-water gas transfer. *Journal of Geophysical Research: Oceans*, 106(C5): 9385–9391. DOI: https://doi.org/10.1029/2000JC000262

Zappa, CJ, Asher,W, Jessup, A, Klinke, J and **Long, S.** 2004. Microbreaking and the enhancement of air-water transfer velocity. *Journal of Geophysical Research: Oceans*, 109(C8). DOI: https://doi.org/10.1029/2003JC001897

Zappa, CJ, McGillis, WR, Raymond, PA, Edson, JB, Hintsa, EJ, Zemmelink, HJ, Dacey, JW and **Ho, DT.** 2007. Environmental turbulent mixing controls on air-water gas exchange in marine and aquatic systems. *Geophysical Research Letters*, 34(10). DOI: https://doi.org/10.1029/2006GL028790

Zavarsky, A, Goddijn-Murphy, L, Steinhoff, T and **Marandino, CA.** 2018. Bubble-mediated gas transfer and gas transfer suppression of dms and co2. *Journal of Geophysical Research: Atmospheres*, 123(12): 6624–6647. DOI: https://doi.org/10.1029/2017JD028071

Zhao, D, Toba, Y, Suzuki, Y and **Komori, S.** 2003. Effect of wind waves on air–sea gas exchange: proposal of an overall co2 transfer velocity formula as a function of breaking-wave parameter. *Tellus B*, 55(2): 478–487. DOI: https://doi.org/10.3402/tellusb.v55i2.16747

TO CITE THIS ARTICLE:
Li, S, Babanin, AV and Guan, C. 2023. Dimensionless Parameterizations of Air-Sea CO_2 Gas Transfer Velocity on Surface Waves. *Tellus B: Chemical and Physical Meteorology*, 75(1), 1–12. DOI: https://doi.org/10.16993/tellusb.1867

Submitted: 08 December 2022 **Accepted:** 20 March 2023 **Published:** 11 April 2023